# SITE AMPLIFICATION FORMULA FOR SEISMIC ZONATION BASED ON DOWNHOLE ARRAY RECORDS DURING STRONG EARTHQUAKES

**T. Kokusho[1] and K. Sato[2]**

[1] *Professor, Dept. of Civil Engineering , Chuo University, Tokyo. Japan*

[2] *Ex-graduate Student, Ditto*

*Email: kokusho@civil.chuo-u.ac.jp*

**ABSTRACT :**

Site amplification essential for seismic zonation is defined here as a peak value of spectrum ratio between ground surface and a base layer. The amplification was investigated using surface and base accelerations recorded in a number of KiK-net downhole arrays in Japan during three recent destructive earthquakes. An important task was to determine the spectral amplifications relative to outcropping motions. Based on soil investigation data available for individual arrays, theoretical amplifications consistent with the peak amplifications of the array records were calculated corresponding to the outcropping motions. A good and unique correlation was found between the peak amplification thus obtained and S-wave velocity ratio, defined as S-wave velocity in a base layer divided by average S-wave velocity, $\overline{Vs}$ for different sites and different earthquakes. The value of $\overline{Vs}$ was evaluated from fundamental mode frequency and a thickness of equivalent surface layer in which peak amplification was exerted. The conventional parameter $Vs_{30}$; averaged shear wave velocity in the top 30m often used in current practice, showed poorer correlation than $\overline{Vs}$ with the obtained amplifications. It is suggested that $\overline{Vs}$ may be determined not only from Vs-logging data but also from microtremor measurements.

**KEYWORDS:** seismic amplification, Vs- ratio, multi-reflection theory, seismic zonation, base layer

## 1. INTRODUCTION

Site amplification is defined between ground surface and bedrock and depends on several factors; the composition of soil layers, S-wave velocities, soil densities, internal damping of the individual layers. Furthermore, the potentially significant effect of strain-dependent nonlinear properties on site amplification in soft soils during strong earthquakes has to be considered (Finn 1991).

Among the influencing factors, a ratio of S-wave velocity between the base layer and surface soil is of utmost importance. Shima (1978) found that the analytically calculated site amplification is almost linearly related to the ratio of S-wave velocity of the surface top layer to that of base layer despite the difference in intermediate soil layers. This indicates that if S-wave velocity of the base layer is assumed relatively unchanged over a wide area, relative amplification between different localities can be obtained solely from the S-wave velocities in the surface layer. Considering that the top layer, sometimes very thin, may not always represent seismic amplification properly, several investigators, Joyner et al. (1981), Joyner and Fumal (1984), Midorikawa (1987) and Borcherdt et al. (1991) employed S-wave velocity averaged over surface soils spanning from the ground surface to a depth of 30 m, $Vs_{30}$, as a key parameter to evaluate the relative amplification. They found $Vs_{30}$ to be an acceptably reliable index of relative amplification.

In order to evaluate site amplification from a base layer to ground surface, NIED (National Research Institute for Earth Science and Disaster Prevention, Japan) deployed several hundreds of vertical array strong motion recording systems called KiK-net all over Japan after the 1995 Kobe earthquake. The system comprises a pair of 3D accelerometers at ground surface and base layer. The observed records together with associated geological and geotechnical data are easily accessible by international researchers at the web site; http://www.kik.bosai.go.jp/kik/.

In general, there can be two different seismic array systems to measure the site amplification between ground surface and base layer as illustrated in Figs.1(a) and (b). One is a surface array system (a) consisting of a set of surface seismometers on different surface geologies in a relatively small area with a common base layer. Seismic records $2A_s$ on a surface soil and $2A_b$ on outcropping base layer allow to directly evaluate site amplification between the two different geologies $2A_s$ /$2A_b$ if incident seismic wave $A_b$ is assumed basically the same in that area. The other is a vertical array system (b) consisting of surface and down-hole seismometers at the same place. This can evaluate site amplification exactly at the same location, though some modification is necessary to extract the outcrop motion $2A_b$ from observed base motion ($A_b$+$B_b$) which is more or less contaminated by downward wave $B_b$ from overlying layers.

In this research, spectrum amplifications are evaluated from strong motion records obtained by the KiK-net vertical arrays during 3 strong earthquakes occurred in recent years in Japan. The Fourier spectrum ratio $2A_s$/($A_b$+$B_b$) between the two measured motions at surface and base are first calculated. It is then used to modify the theoretical transfer function $2A_s$ /$2A_b$ based on multiple reflection theory of 1-dimensional SH waves by removing the effect of downward wave $B_b$ on the measured motion at the base layer. The peak amplifications of the modified transfer functions $2A_s$ /$2A_b$ are then correlated with S-wave velocity ratios between base and surface. The procedure for determining the appropriate S-wave velocity in a surface layer of appropriate thickness will be described later.

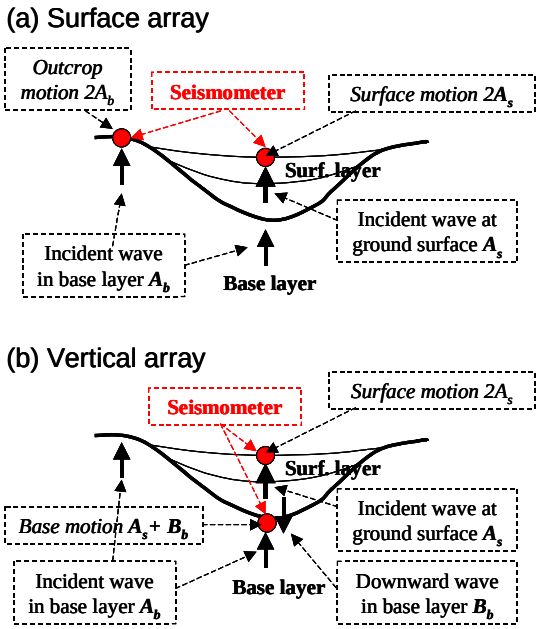


Figure 1 Two seismic array systems (a) & (b) to measure site amplification between ground surface and base layer.

## 2. EARTHQUAKE RECORDS AND AVERAGE S-WAVE VELOCITY

Three strong earthquakes studied here are EQ1: the 2003 Tokachi-Oki earthquake ($M_J$=8.0), EQ2: the 2004 Niigataken-Chuetsu earthquake ($M_J$=6.8) and EQ3: the 2005 Fukuokaken-Seihou-Oki earthquake ($M_J$=7.0). Here, $M_J$ is the earthquake magnitude on the Japanese Meteorological Agency scale and nearly equivalent to the Richter Magnitude. Strong motion records at 20 sites with maximum acceleration ($Acc_{max}$) higher than 200 cm/s$^2$ in EQ1, at 15 sites with $Acc_{max}$ >100 cm/s$^2$ in EQ2, and at 11 sites with $Acc_{max}$ >100 cm/s$^2$ in EQ3 are used in this research. In Fig.2, the maximum accelerations at the ground surface and at the base layer for all the sites are plotted along the vertical and horizontal axes, respectively. The surface values, spanning from 100 to 600 gals, are mostly 2-8 times larger than the base values.

The depth of the down-hole seismometer in the vertical arrays used here varies from 100 m to 330 m. The base layer is defined here as a layer where down-hole seismometer is installed. The S-wave velocity $Vs_b$ at a site is normally stable in the depth and does not drastically change between neighboring layers. However, it regionally diverges from $Vs_b$ =400 m/s to 3000 m/s among different sites measuring the 3 earthquakes; the smallest for EQ1 and the largest for EQ3. In a good contrast, the surface velocity $Vs$ is lower than 400 m/s (mostly around 200 m/s) with only two exceptions for all the recording sites used here (Kokusho and Sato 2008).

Fourier spectrum ratios were computed between ground surface and base layers. Typical results for main shock and

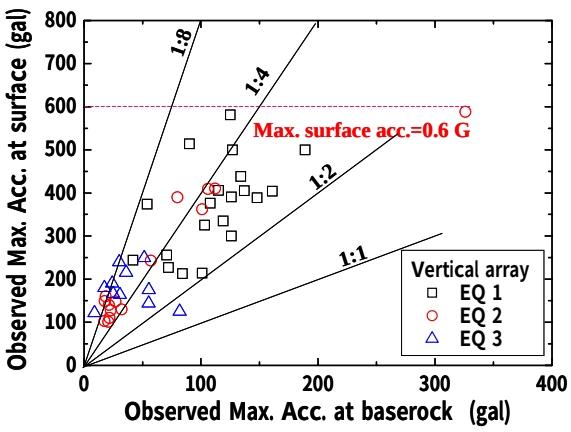


Figure 2 S-wave velocities compared between top layer and base layer for all vertical array sites.

several aftershocks of EQ1 at 2 sites are exemplified for the EW direction in Figs.3(a) and (b). There is a clear difference in the spectrum ratio between main shock and aftershocks in both sites reflecting the effects of the strain-dependent soil properties which result in nonlinear site response to strong shaking. In order to specify soil layers generating peak frequencies in the spectrum ratios, fundamental mode frequencies of layered soil systems $f_1$ were calculated by the following formula based on soil logging data for the two sites along with S-wave velocities of individual layers.

$$f_1 = 1\Big/\left[4\sum_{i=1}(H_i/Vs_i)\right] \qquad (1)$$

Here, $H_i$ and $Vs_i$ are the thickness and the S-wave velocity of the *i*-th layer numbered from the top, and the summation is implemented layer by layer down to the base. This frequency corresponds to a wave length which is equal to 4 times the layer thickness. The calculated frequency is compared one by one with the peak frequency in the spectrum ratio of observed motions such as in Figs.3(a) and (b) to identify equivalent surface layers of thickness $H_s = \sum_{i=1} H_i$ consisting of one or more layers generating the fundamental mode frequency calculated by Eq.(1). Note that there can be multiple equivalent surface layers in the same site corresponding to individual peak frequencies. The value of $f_1$ by Eqs.(1) is listed layer by layer together with equivalent surface layers thus identified. Thus, some of the peak frequencies in spectrum ratios may be explained by the fundamental modes of equivalent surface layers, though there are unidentified peaks probably because higher order modes which cannot be considered by Eq.(1) are actually involved.

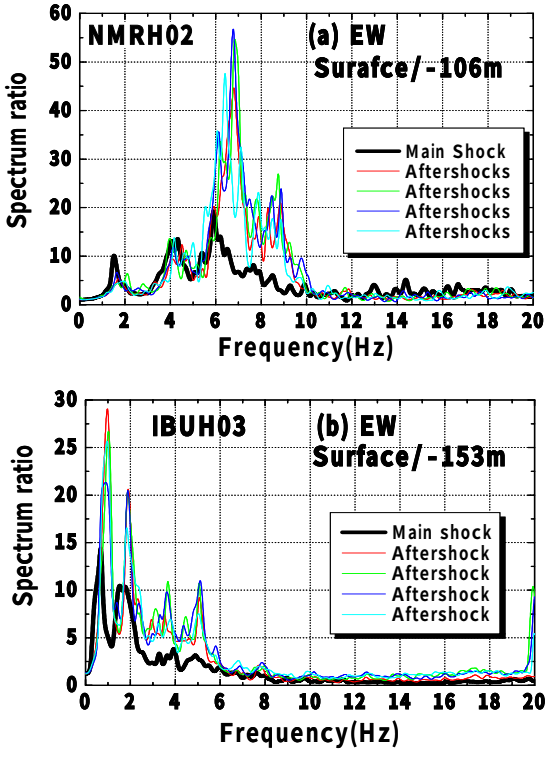


Figure 3 Spectrum ratios versus frequency in EW and NS directions for main shock and aftershocks at NMRH02 in EQ1.

In Fig.4, the peak frequencies $f_1$ calculated by Eq.(1) based on given soil data are taken in the horizontal axis to compare with the frequencies $f^*$ identified in the observed spectrum ratios for the main shock and aftershocks in the vertical axis for the recording sites of EQ3. Most of the plots corresponding to 1st peaks and higher order peaks concentrate along the diagonal line of $f^* = f_1$ and within the two lines of $f^* = 0.7 f_1$ and $f^* = 1.2 f_1$. Thus, it may be said that there exists a satisfactory correspondence between the fundamental mode frequency of soil models $f_1$ based on Eq.(1) and the peak frequency $f^*$ observed in spectrum ratios irrespective of the order of peaks, although there can be some discrepancies partly because Eq.(1) is not a rigorous formula for the fundamental mode frequency but just an approximation. It further implies that major peaks in the observed spectrum ratios may be explained by the fundamental mode of equivalent surface layers consisting of one or more layers near ground surface.

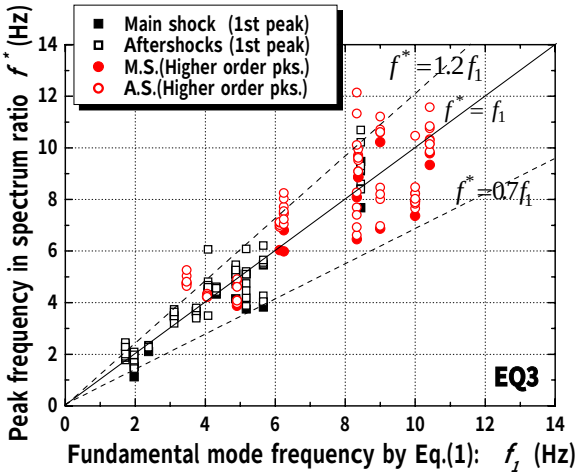


Figure 4 Peak frequencies calculated by Eq.(1) based on soil data compared with identified frequencies in observed spectrum ratios for main shock and aftershocks for all sites in EQ3.

The average S-wave velocity $\overline{Vs}$ for each equivalent surface layer can be calculated from the fundamental

mode frequency $f_1$ and its thickness $H_s = \sum_{i=1} H_i$ as

$$\overline{Vs} = 4H_s f_1 \qquad (2)$$

Thus, average S-wave velocity directly related with major peaks of the spectrum ratio can be reasonably determined by Eq.(2).

## 3. SPECTRUM RATIO BETWEEN SURACE AND BASE

Fourier spectrum ratios between surface and base $2A_s/(A_b+B_b)$ of observed motions were calculated. In Fig.5, the peak amplifications for the main shock are plotted with solid symbols versus $Vs_b/\overline{Vs}$, where $\overline{Vs}$ is the average S-wave velocity of the equivalent surface layer calculated by Eq.(2) as previously explained according to individual peak frequencies. Despite some data scatters, a correlation can be recognized in Fig.5, in which the amplification is almost linearly dependent on $Vs_b/\overline{Vs}$ at least up to $Vs_b/\overline{Vs} \approx 8$, indicating that $\overline{Vs}$ is a good parameter to evaluate the peak amplifications of $2A_s/(A_b+B_b)$. The peak amplifications of the aftershocks of EQ1 observed at the same sites are also plotted with open marks in Fig.5. Obviously, the amplifications, though quite variable depending on sites and individual aftershocks, are much larger than those of the main shock in most of the sites, indicating a strong influence of strain-dependency in soil properties on the amplification mechanism of measured motions between surface and base.

In seismic zonation of an area resting on a common base layer, a transfer function between ground surface and an outcropping base layer $2A_s/2A_b$ is used, in place of $2A_s/(A_b+B_b)$. Hence, the problem is how to evaluate $2A_s/2A_b$ based on measured motions in the vertical arrays. A procedure chosen here is as follows.

1) First, a theoretical transfer function, $2A_s/(A_b+B_b)$ is calculated for each site based on the multi-reflection theory. Among soil properties needed, the S-wave velocities of individual layers are given by in situ logging test results available in the website and soil densities are decided from previous experiences based on given soil types. The damping ratio $D$, assumed as non-viscous or frequency-independent, is tentatively set as 2.5% in all layers.
2) Then, the theoretical transfer function is compared with measured spectrum ratio as exemplified in Fig.6. In order to make the comparison fair, the same Parzen window of 0.3 Hz is also used in computing $2A_s/(A_b+B_b)$ theoretically. If a peak in the transfer function can be found at about the same frequency in the spectrum ratio of observed motions, it is identified as the corresponding peak, and the damping ratio, assumed as $D$=2.5% previously, is modified by the following equation to have the same peak value, $D = Q_1/Q_2 \times 2.5$ (%), where $Q_1$ is the peak amplitude of the theoretical transfer function, and $Q_2$ is that of spectrum ratio based on the actual records.

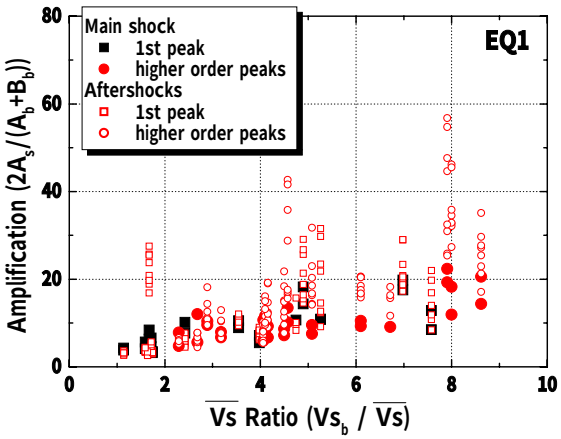


Figure 5 Peak amplitudes of 2*As*/ ($A_b$+ $B_b$) for main shock and aftershocks in vertical array sites of EQ1 versus average S-wave velocity ratios

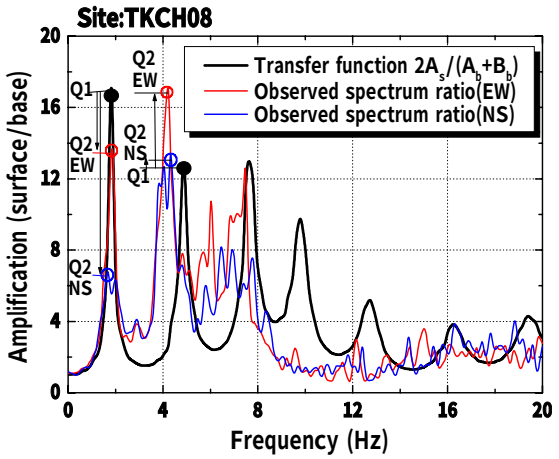


Figure 6 Comparison of transfer functions, $2A_s/(A_b+B_b)$ and spectrum ratio of observed motions at the same site.

Not only the 1st peak but also the higher order peaks are compared in this manner if possible, and the values of *D* in the two directions, EW and NS are averaged. The *D*-value thus evaluated is considered to represent average amplification in the upper ground above the base layer and also more or less reflecting strain-dependency of soil damping.

3) Next, another theoretical transfer function $2A_s/2A_b$ is computed using the modified damping ratio *D* based on the same soil layers system. Fig.7 exemplifies the two transfer functions $2A_s/(A_b+B_b)$ and $2A_s/2A_b$, which possess almost identical peak frequencies. However, in some site conditions, peak frequencies of the two functions can be widely different. In such cases, peak frequencies of $2A_s/2A_b$ are compared again with fundamental mode frequencies associated with a layered soil system calculated by Eq.(1) and equivalent surface layers, and associated average S-wave velocities by Eq.(2) are determined again. In cases where such peaks are not found at all comparable between the computed transfer function and the peak frequencies calculated from Eq.(1), that data is omitted in the following data reduction. The peak amplification for the function $2A_s/2A_b$ thus evaluated using the modified damping ratio should be equal to the peak value in the spectrum ratio of observed motions between ground surface and base layer if the effect of downward wave into the base layer could have been removed. In this way, the peak amplification of $2A_s/2A_b$ between surface and base, to be used for seismic zonation study for surface ground resting on common base layer, can be obtained using the vertical array records.

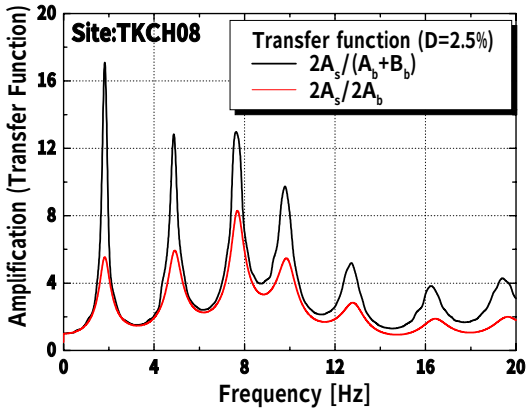


Figure 7 Comparison of transfer functions, $2A_s/(A_b+B_b)$ and $2A_s/2A_b$, at the same site.

## 4. S-WAVE VELOCITY RATIO VERSUS AMPLIFICATION FOR ZONATION

In Fig.8, the peak amplifications for $2A_s/2A_b$ computed by the methodology mentioned above for vertical array sites of EQ1 are plotted versus average S-wave velocity ratios $Vs_b/\overline{Vs}$ for the main shock with a solid symbol. The velocity ratio $Vs_b/\overline{Vs}$ is defined here as a division of the S-wave velocity at a base layer $Vs_b$ by the velocity $\overline{Vs}$ evaluated by Eq.(2) from the fundamental mode frequencies of Eq.(1) based on S-wave logging data at each site. A clear correlation can be recognized between the peak amplification and the velocity ratio both for 1st and higher order peaks, despite some scatters of data points.

Four aftershock records of EQ1 is also analyzed in the same way and the results are plotted in Fig.8 with an open symbol. The difference in amplification $2A_s/2A_b$ between main shock and aftershocks is evidently smaller than that for $2A_s/(A_b+B_b)$ shown in Fig.5. In order to basically understand the different influence of strain-dependent nonlinear soil properties on the amplifications on the two kinds of spectrum ratios, $2A_s/2A_b$ and $2A_s/(A_b+B_b)$, a simple 2-layers system of a surface layer and a base layer (infinite thickness) was considered (Kokusho and Sato 2008), which indicates that nonlinear properties make a great difference in the peak frequencies, though the difference in the peak amplifications is less pronounced in $2A_s/2A_b$ than in $2A_s/(A_b+B_b)$ for the 1st peak in particular. That is

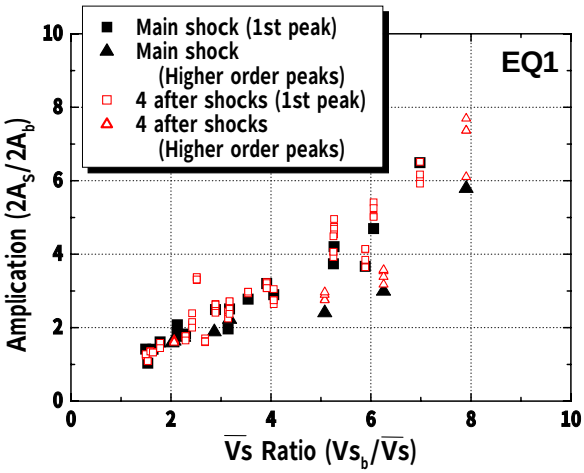


Figure 8 Peak amplitudes of $2A_s/A_b$ for main shock and aftershocks of EQ1 versus average S-wave velocity ratios.

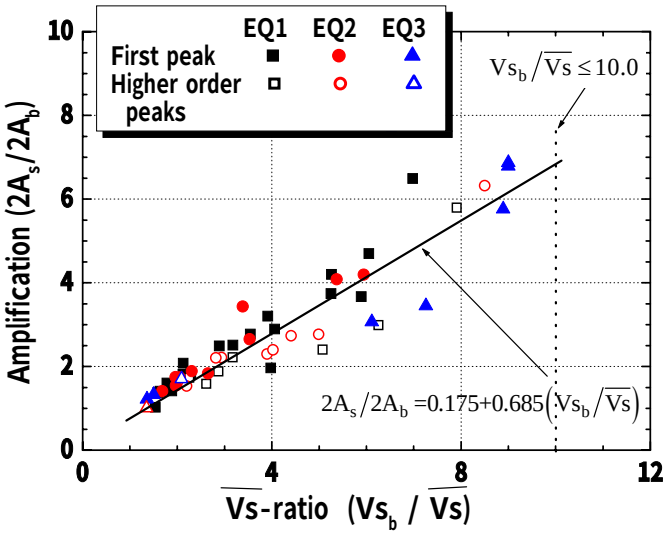


Figure 9 Peak amplitudes of $2A_s/2A_b$ for main shocks of 3 earthquakes versus average S-wave velocity ratios $Vs_b/\overline{Vs}$ proposed here and approximation by empirical equation.

because, under the paramount effect of radiation damping, the difference in the amplification $2A_s/2A_b$ due to strain-dependent properties becomes less conspicuous. Furthermore, the impedance ratio, which becomes smaller with degraded modulus or degraded S-wave velocity in the surface layer, tends to give larger amplification compensating the effect of increased damping ratio during strong earthquakes. Thus, the difference in soil nonlinearity between the main shock and aftershocks tends to have smaller influence on the amplification in $2A_s/2A_b$ than in $2A_s/(A_b+B_b)$ as demonstrated in the comparison of Figs.5 and 8.

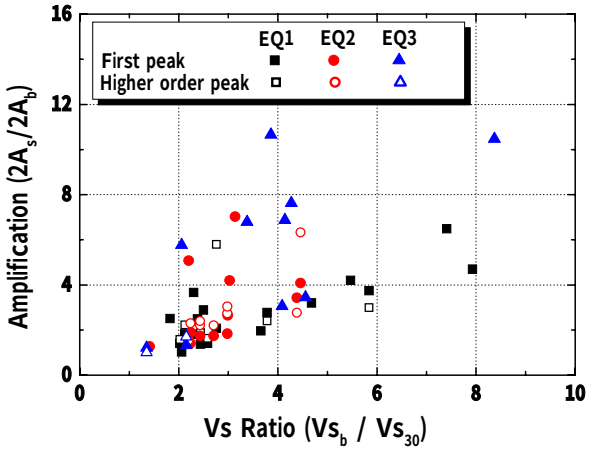


Figure 10 Peak amplitudes of $2A_s$/ $2A_b$ for main shocks of 3 earthquakes versus average S-wave velocity ratios $Vs_b/Vs_{30}$ for surface soils of top 30m.

Fig.9 shows the relationship between the peak amplitude corresponding to $2A_s/2A_b$ and the velocity ratio $Vs_b/\overline{Vs}$ plotted for main shocks of the three earthquakes investigated here. Totally 54 data points (37 for the 1st peak and 17 for the higher order peaks) from 37 recording sites are included in this chart (2 data points in which $Vs_b/\overline{Vs}$ =16 and 21 are excluded here), and a large number of plots are overlapping in the zone of $Vs_b/\overline{Vs}$ <4.0. Quite remarkably, the plots show a fairly good correlation including both 1st and higher order peaks (the regression coefficient = 0.91) despite differences in various influencing factors associated with the three earthquakes; namely, dominant frequency, shaking duration, regional geological difference, etc.

In the current practice of seismic zonation, the S-wave velocity ratio defined as $Vs_b/Vs_{30}$, where $Vs_{30}$ = averaged S-wave velocity over top 30 m from ground surface, is sometimes used (Joyner and Fumal 1984, Midorikawa 1987) instead of the definition proposed here as $Vs_b/\overline{Vs}$. In Fig.10, the same peak amplitudes corresponding to $2A_s/2A_b$ are plotted versus the velocity ratio, $Vs_b/Vs_{30}$. Here, $Vs_{30}$ (m/s) is calculated by the equation; $Vs_{30}=30/T_{30}$ in which $T_{30}$ (s) is the traveling time of S-wave in the top 30 m based on soil logging data. Obviously, the correlation becomes poorer than in Fig.9, though it does not look so bad for a single earthquake such as EQ1 in particular. Inconsistency in plots between 1st and higher order peaks is also

evident. This indicates the importance to define the average S-wave velocity properly by identifying site by site the equivalent surface layer in which individual peak amplifications are exerted.

The data points in Fig.9 satisfying the condition $Vs_b/\overline{Vs} \le 10.0$, which may be applicable to most site conditions, can be approximated by a simple linear function;

$$2A_s/2A_b = 0.175 + 0.685\left(Vs_b/\overline{Vs}\right) \qquad (3)$$

It is readily understood that, for a non-dissipative uniform ground, the value of $2A_s/2A_b$ can be obtained as 1.0. However, in the uniform ground of $Vs_b/\overline{Vs} = 1.0$, $2A_s/2A_b = 0.86$ is extrapolated from Eq.(3). This gap may be justified considering the effect of soil damping on the wave propagation from the base layer to the surface. Eq.(3) may be conveniently used because of its applicability to a wide variety of base layers with $Vs_b$ =400 m/s to 3000 m/s.

The relative amplification for the same seismic motion in an area overlying a common base layer is readily evaluated. The procedure is as follows;

1) Find a layer boundary in wave logging data where S-wave velocity clearly changes, above which the upper layers will potentially vibrate in the fundamental mode and hence considered as the equivalent surface layer. Calculate the average S-wave velocity of the equivalent surface layer $\overline{Vs}$ by Eq.(2).
2) If there is no S-wave logging data available, carry out micro-tremor measurement, and decide fundamental frequency $f_1$ of a site using H/V spectrum ratios (Nakamura 1989). On the other hand, estimate the thickness of a soft soil or Holocene layer $H$ where the fundamental frequency is exerted, which is sometimes possible based on geological maps or high-density soil logging data available in city areas. Then, the average S-wave velocity can be calculated by $\overline{Vs} = 4Hf_1$.
3) Calculate the S-wave velocity ratio $Vs_b/\overline{Vs}$ from $Vs_b$ of the common base layer and $\overline{Vs}$ obtained above for individual site conditions.
4) Comparing the amplifications by Eq.(3) at two different sites gives the relative amplification between them. To be precise, the amplification by Eq.(3) is slightly changeable depending on the value of $Vs_b$ to be chosen among different base layers in the two sites, though its effect is ignorable for design purposes.

In the above, seismic response of ground is evaluated based on linear transfer function assuming that soil nonlinearity exerted during earthquakes is not so considerable. This assumption may not hold in those sites, such as Port Island during the 1995 Kobe earthquake (Kokusho et al. 2005). Strong soil nonlinearity by extensive liquefaction occurred there may have completely changed the soil system not to be able to justify the methodology employed here.

Finally, it should be noted again that the depths of the down-hole seismometers used in this study are 100~330 m. If a base layer considered becomes much deeper than this range, wave attenuation in the deep ground tends to be more pronounced, leading to lower amplification than proposed here. Hence, further research is needed to clarify seismic amplification of a soil ground of a greater depth.

## 5. CONCLUSIONS

In studying seismic amplification between ground surface and base layer using KiK-net records of recent 3 strong earthquakes occurred in Japan, average S-wave velocity $\overline{Vs}$ for equivalent surface layer corresponding to each peak of Fourier spectrum ratio was introduced from S-wave logging data. Then, a velocity ratio $Vs_b/\overline{Vs}$ was defined by dividing S-wave velocity at a base layer $Vs_b$ by the average velocity $\overline{Vs}$ in the equivalent surface layer. The peak amplifications of the spectrum ratios were calculated and correlated with the velocity ratio. The spectrum amplifications relative to outcrop motions to be used for seismic zonation of surface ground resting on common base layer were computed from theoretical transfer functions and adjusted to be consistent with the peak amplifications of the array records.

The major findings in this research are;

1) Spectrum peak amplifications of $2A_s/(A_b + B_b)$ for measured motions between surface and base layers can be evaluated with small data dispersions by using the velocity ratio $Vs_b/\overline{Vs}$.
2) The strain-dependent soil nonlinearity tends to have a greater effect on the peak amplifications of

$2A_s/(A_b+B_b)$ for measured motions than those of $2A_s/2A_b$ for outcrop motions.

3) The spectrum peak amplifications of $2A_s/2A_b$ for outcrop motions plotted versus the velocity ratios $Vs_b/\overline{Vs}$ show a good correlation with a small data dispersion between the peak amplification and the velocity ratio both for 1st and higher order peaks, despite differences in influencing factors of the three earthquakes.
4) If the same peak amplifications are plotted versus velocity ratios conventionally defined as $Vs_b/Vs_{30}$ ($Vs_{30}$ = average velocity for top 30m layer) sometimes used in the current seismic zonation practice, the correlation becomes poorer, indicating the importance to define the average S-wave velocity adequately by identifying a site-specific equivalent surface layer in which peak amplifications are exerted.
5) The correlation obtained here is formulated by Eq.(3) under the condition $Vs_b/\overline{Vs} \le 10$, which may be conveniently used for evaluating relative amplification in seismic zonation study covering an area resting on a common base layer having arbitrary S-wave velocity, $Vs_b$.
6) The velocity $\overline{Vs}$ of the equivalent surface layer can be evaluated from Vs logging data, or if it is unavailable, can be decided from fundamental mode frequency $f_1$ of a site using H/V spectrum ratios in micro-tremor measurements together with the thickness of soft soil or Holocene layer $H$ by $\overline{Vs} = 4Hf_1$.

## ACKNOWLEDGMENTS

NIED (National Research Institute for Earth Science and Disaster Prevention) in Tsukuba, Japan, who generously provided KiK-net data through the internet, is gratefully acknowledged. The great efforts in data reduction of voluminous KiK-net records by graduate and undergraduate students of Civil Engineering Department in Chuo University are also very much appreciated.

## REFERENCES

Borchert, R. D., Wentworth, C. M., Janssen, A., Fumal, T. and Gibbs, J. (1991): Methodology for Predictive GIS Mapping of Special Study Zones for Strong Ground Shaking in San Francisco Bay Region. *Proc. 4th International Conference on Seismic Zonation*, Vol.3, 545-552.

Finn, W. D. L. (1991): Geotechnical engineering aspects of microzonation, *Proc. 4th International Conference on Seismic Zonation*, Vol.1, 199-259.

Joyner, W. B. Warrick, R. E. and Fumal, T. E. (1981): The effect of Quaternary alluvium on strong ground motion in the Coyote Lake, California, earthquake of 1979: *Bulletin, Seismological Society of America*, Vol.71, 1333-1349.

Joyner, W. B. and Fumal, T. E. (1984): Use of measured shear-wave velocity for predicting geologic site effects on strong ground motion, Proc. of 8th World Conference on Earthquake Engineering, Vol.2, pp.777-783.

Kokusho, T., Aoyagi, T. and Wakunami, A. (2005): In situ soil-specific nonlinear properties back-calculated from vertical array records during 1995 Kobe Earthquake, *Journal of Geotechnical and Geoenvironmental Engineering*, ASCE, Vol.131, No.12, 1509-1521.

Kokusho, T. and Sato, K. (2008): Surface-to-base amplification evaluated from KiK-net vertical array strong motion records, Soil Dynamics and Earthquake Engineering, 2008.

Midorikawa, S. (1987): Prediction of iso-seismal map in the Kanto Plain due to hypothetical earthquake. *Journal of Structural Engineering*, Vol.33B, 43-48, (in Japanese).

Nakamura, Y. (1989): A method for dynamic characteristics estimation of subsurface using microtremor on the ground surface, *QR of Railway Technical Research Institute*, Vol.30, 25-33.

Shima, E. (1978): Seismic Microzoning map of Tokyo. *Proc. Second Inter. Conf. on Microzonation* (1), 433-443.